

# IceCube Constraints on Fast-Spinning Pulsars as High-Energy Neutrino Sources

Ke Fang<sup>a</sup>, Kumiko Kotera<sup>b</sup>, Kohta Murase<sup>c</sup> and Angela V. Olinto<sup>d</sup>

<sup>a</sup>Department of Astronomy, University of Maryland, College Park, MD, 20742, USA

<sup>b</sup>Institut d'Astrophysique de Paris, UMR 7095 - CNRS, Université Pierre & Marie Curie, 98 bis boulevard Arago, 75014, Paris, France

<sup>c</sup>Department of Physics; Department of Astronomy & Astrophysics; Center for Particle and Gravitational Astrophysics, The Pennsylvania State University, PA 16802, USA

<sup>d</sup>Department of Astronomy & Astrophysics, Kavli Institute for Cosmological Physics, The University of Chicago, Chicago, IL 60637, USA.

**Abstract.** Relativistic winds of fast-spinning pulsars have been proposed as a potential site for cosmic-ray acceleration from very high energies (VHE) to ultrahigh energies (UHE). We re-examine conditions for high-energy neutrino production, considering the interaction of accelerated particles with baryons of the expanding supernova ejecta and the radiation fields in the wind nebula. We make use of the current IceCube sensitivity in diffusive high-energy neutrino background, in order to constrain the parameter space of the most extreme neutron stars as sources of VHE and UHE cosmic rays. We demonstrate that the current non-observation of  $10^{18}$  eV neutrinos put stringent constraints on the pulsar scenario. For a given model, birthrates, ejecta mass and acceleration efficiency of the magnetar sources can be constrained. When we assume a proton cosmic ray composition and spherical supernovae ejecta, we find that the IceCube limits almost exclude their significant contribution to the observed UHE cosmic-ray flux. Furthermore, we consider scenarios where a fraction of cosmic rays can escape from jet-like structures piercing the ejecta, without significant interactions. Such scenarios would enable the production of UHE cosmic rays and help remove the tension between their EeV neutrino production and the observational data.

**Keywords:** cosmic ray acceleration, neutron star, pulsar, supernova, ultrahigh energy cosmic rays, very high energy cosmic rays

---

## Contents

<b>1</b>	<b>Introduction</b>	<b>1</b>
<b>2</b>	<b>UHECRs and High-energy neutrinos from young neutron stars</b>	<b>3</b>
2.1	Particle injection and acceleration	3
2.2	Radiation backgrounds in the nebula region and in the supernova ejecta	4
2.3	Surrounding ejecta and escape (baryonic background)	7
2.4	Neutrino production and diffuse flux	8
2.5	Comparison between radiative and hadronic background effects	11
<b>3</b>	<b>Parameter scan and the viable neutron stars</b>	<b>12</b>
<b>4</b>	<b>In presence of jet-like structures</b>	<b>14</b>
<b>5</b>	<b>Discussion, conclusions</b>	<b>16</b>

---

## 1 Introduction

Galactic accelerators are likely responsible for the dominant component of cosmic rays observed on Earth (below  $10^{15}$  eV), given their containment by the Galactic magnetic field (e.g., [1–3]). The recent gamma-ray observations support that the main sources of these Galactic cosmic rays are supernova remnants [4–6]. A transition is expected to occur at higher energies (around  $10^{17-18}$  eV), and cosmic rays should originate in – yet unidentified – extragalactic sources. The known Galactic objects do not possess the required energetics to produce cosmic rays above  $10^{18}$  eV. Besides, the presence of a source in the Galaxy contributing at these energies would induce a signature in the large-scale anisotropy of the arrival directions of cosmic rays, that is not observed. Measurements with the Auger Observatory and the Telescope Array are already constraining the Galactic-extragalactic transition energy and models of the Galactic magnetic field [7–9].

At the highest energies, the possible candidate sources have been progressively narrowed down to a handful of objects over the last decades, but the major culprit has not been yet identified. Among the most promising sources, active galactic nuclei (AGN) with their black holes, jets, hotspots, and flares, as well as gamma-ray bursts (GRBs), including low-luminosity GRBs associated with trans-relativistic supernovae, are heavily plebiscited (see e.g., review [10] and references therein). A contender that was introduced early on by Refs. [11–13] and has

been resuscitated more recently by Refs. [14–17] are magnetized and fast-spinning neutron stars. These objects combine many advantages: their rotation speed endows them with a large energy reservoir ( $E_{\text{rot}} \sim 2 \times 10^{52} \text{ erg } I_{45} P_{-3}^{-2}$ , with  $I$  the star inertial momentum and  $P$  its spin period<sup>1</sup>, for an isolated new-born pulsar spinning close to the disruption limit), and their population density ( $\dot{n}_s \sim 10^{-4} \text{ Mpc}^{-3} \text{ yr}^{-1}$  [18]) is high enough to allow a comfortable total energy budget. The energy injected into UHECRs is of order  $\dot{\mathcal{E}}_{\text{UHECR}} \sim 0.5 \times 10^{44} \text{ erg Mpc}^{-3} \text{ yr}^{-1}$  [19, 20], which implies that a fraction of order  $10^{-4}$  of the neutron star population is required to achieve the ultrahigh energy cosmic ray (UHECR) flux level.

Within the zoo of neutron stars, those with extremely strong surface dipole fields of  $B \sim 10^{15} \text{ G}$ , which are often called *magnetars* (see [21–23] for reviews), have attracted particular attention because of their energetics [13–15]. This subpopulation, the existence of which was predicted in the 90s [25], is accepted as the explanation to the observed Soft Gamma Repeaters and Anomalous X-ray Pulsars [26–28].

Neutron stars are believed to be the byproducts of supernovae explosions. It is thus likely that, at the early stage of the neutron star life, when it is able to supply enough energy to accelerate particles to ultrahigh energies, it is surrounded by the radiatively and baryonically dense supernova ejecta. Assuming that particles can be successfully accelerated within the neutron star wind or nebular region, they will have to cross this interface, as well as the dense supernova ejecta, on their way to the interstellar medium. In Ref. [16], we demonstrated that for magnetars, the energy losses experienced by particles during their flight in the supernova ejecta did not allow their escape at ultrahigh energies, unless the ejecta mass was considerably lower than for standard core-collapse supernovae, or if a mechanism such as a jet was invoked to pierce the envelope. Indeed, magnetars spin down faster than more mildly magnetized stars, and the highest energy particles are produced when the surrounding ejecta is still too opaque to let them escape.

Magnetars are thus not necessarily favored to produce cosmic rays at the highest energies. They could be contributing however at energies below  $\sim 10^{18-19} \text{ eV}$ . In this energy range, the composition measured by the current experiments indicate that protons are dominant [29, 30].

The interactions of cosmic rays within the nebula or supernova ejecta regions should lead to the generation of secondary particles, including high energy neutrinos, which has been suggested as a very powerful test of newborn pulsar scenarios for UHECRs [14]. The guaranteed level of neutrinos expected for a pulsar population fitting the Auger data (both spectrum and composition) was calculated in Ref. [31]. We demonstrated there that this flux would be observable by IceCube within the next ten years.

In this work, we make use of the current IceCube sensitivity in neutrinos, in order to constrain the parameter space of the most extreme neutron stars as extragalactic sources of cosmic rays, focussing on the particle energy range above  $10^{17} \text{ eV}$ . As discussed in this study, this range corresponds indeed to the peak of the produced neutrino flux. We demonstrate that the current non-observation of neutrinos in the EeV range radically shrinks the range of parameters allowed for magnetars that would efficiently produce very high-energy cosmic rays, and almost exclude any contribution from these sources. For higher energies, as mentioned above, either a low mass supernova ejecta or a jet-like structure is needed to

---

<sup>1</sup>Here and in what follows, quantities are labelled  $Q_x \equiv Q/10^x$  in cgs units unless specified otherwise.

let particles escape without too much damage. We show that even within these scenarios, the constraints imposed by the level of neutrinos at EeV energies still partially constrain magnetars as sources of UHECRs.

We give in Section 2 an overview of the UHECR production issues (ion injection, acceleration and escape) related to neutron stars and their surrounding nebula and supernova ejecta. We estimate the corresponding neutrino fluxes in Section 2.4. In Section 3, we present our parameter scan over the neutron star pulsation and dipole field, the source birth rate, the efficiency of a jet-like structure, and the particle acceleration efficiency. We discuss our results and conclude in Section 5.

## 2 UHECRs and High-energy neutrinos from young neutron stars

### 2.1 Particle injection and acceleration

Ions (from light to heavy nuclei) can be stripped off the neutron star surface by a combination of strong electric fields and bombardment of particles [32, 33]. The acceleration mechanism of these extracted particles up to ultrahigh energies in neutron star environments is an unclear point of this source scenario. Our poor knowledge of the neutron star magnetospheres, winds, nebulae and termination shocks (at the interface between the wind and the surrounding supernova ejecta) is central to the difficulties encountered in building a detailed acceleration model, consistent with the observations and the leptonic emission counterparts. The features of the radiation due to pairs are themselves challenging to explain, and despite an increasing experimental and theoretical effort been put to understand the working of neutron star outflows and nebular emissions, the community is still struggling to solve fundamental problems (see e.g., reviews by Ref. [34, 35]), such as how and where pairs are been accelerated, or the related problem of electromagnetic to kinetic energy transfer within the wind (the so-called  $\sigma$ -problem).

One certainty however is that neutron stars spin down, and subsequently, their rotational energy is channeled via their winds towards the outer medium. Following Ref. [36], one can calculate that particles of mass number  $A$  in the wind can reach a maximum energy at neutron-star birth

$$E_0 \sim 2.7 \times 10^{20} \text{ eV} A \eta \kappa_4^{-1} P_{i,-3}^{-2} B_{15} R_{\star,6}^3, \quad (2.1)$$

where  $B$  is the dipole magnetic field strength of the star,  $R_\star$  its radius and  $P_i$  the initial spin period. The value of  $\kappa$ , the pair multiplicity, can range between  $10 - 10^8$  in theory (a highly debated quantity, see e.g., [35]). This estimate assumes that the electromagnetic luminosity of the pulsar wind  $L_p \sim 6.6 \times 10^{48} P_{-3}^{-4} B_{15}^2 R_{\star,6}^6 \text{ erg/s}$  is converted into kinetic luminosity  $\dot{N}mc^2$  with efficiency  $\eta \leq 1$ :  $E_0 = \eta L_p / \dot{N}mc^2$ . The particle rest mass power can be written as a function of the Goldreich-Julian rate  $\dot{N}_{\text{GJ}}$  [37]:  $\dot{N}mc^2 \equiv \dot{N}_{\text{GJ}}(2\kappa m_e + Am_p/Z)c^2$  [36].

Note that acceleration to high energies can only happen in the first stages of the life of the neutron star, typically within the spin-down timescale

$$t_{\text{EM}} = \frac{9Ic^3P^2}{8\pi^2B^2R^6} \sim 3.1 \times 10^3 \text{ s} I_{45} B_{15}^{-2} R_{\star,6}^{-6} P_{i,-3}^2. \quad (2.2)$$

If gravitational wave losses are substantial, the star spins down over a timescale

$$t_{\text{GW}} = \frac{5c^5 P^4}{2^{10} \pi^4 G I \epsilon^2} \sim 1.5 \times 10^6 \text{ s } P_{i,-3}^4 I_{45}^{-1} \epsilon_{-4}^2, \quad (2.3)$$

with  $\epsilon$  the ellipticity created by the interior magnetic fields of the star [38–40]. Typically  $\epsilon = \beta R_\star^8 B^2 / (4GI^2) \sim 4 \times 10^{-4} \beta_2 R_{\star,6}^8 B_{15}^2 I_{45}^{-2}$ , where  $\beta$  is the magnetic distortion factor introduced by Ref. [39], which measures the efficiency of the interior magnetic field in distorting the star. This factor depends on the equation of state of the star interior and on its magnetic field geometry. Ref. [39] finds that the value of  $\beta$  can range between 1–10 for perfectly conducting interiors (normal matter), 10–100 for type I superconductors and can reach  $\gtrsim 100$  for type II superconductors (for a detailed study on the connection between magnetars as sources of UHECRs and gravitational waves, see Ref. [15]). We will note

$$t_{\text{sd}} \equiv (t_{\text{EM}}^{-1} + t_{\text{GW}}^{-1})^{-1}. \quad (2.4)$$

In the following, we will place ourselves in a regime where the conversion efficiency of the wind electromagnetic into kinetic luminosity is high enough to achieve ultrahigh energies. Our results remain valid if we relax this assumption, at the cost of a softer injection spectrum that would be produced by the stochastic acceleration to reach the highest energies.<sup>2</sup> Taking into account the neutron-star spin down (assuming a breaking index of 3), we thus consider that cosmic rays are accelerated at a given time  $t$  at energy [12, 13]

$$\begin{aligned} E_{\text{CR}}(t) &= E_0 (1 + t/t_{\text{sd}})^{-1} \\ &\sim 1.3 \times 10^{20} \text{ eV } A \eta \kappa_4 I_{45} B_{15}^{-1} R_{\star,6}^{-3} t_{3.5}^{-1}. \end{aligned} \quad (2.5)$$

Channeling the Goldreich-Julian charge density into particles and taking into account the neutron-star spin down rate, one can write the cosmic-ray injection flux [12, 13]

$$\frac{dN_{\text{CR}}}{dE}(t) = \frac{9}{4} \frac{c^2 I}{ZeBR_\star^3} E_{\text{CR}}(t)^{-1} \left[ 1 + \frac{E_{\text{CR}}(t)}{E_{\text{GW}}} \right]^{-1}, \quad (2.6)$$

where  $E_{\text{GW}}$  is the critical gravitational energy at which gravitational wave and electromagnetic losses are equal. The cosmic-ray luminosity then reads

$$L_{\text{CR}}(t) \equiv E_{\text{CR}}^2 \frac{d^2 N_{\text{CR}}}{dE dt}(t) = \frac{9}{4} \frac{c^2 I}{ZeBR_\star^3} E_{\text{CR}}(t) (t + t_{\text{sd}})^{-1}. \quad (2.7)$$

## 2.2 Radiation backgrounds in the nebula region and in the supernova ejecta

Ultrahigh energy ions can experience photo-pion production or photo-disintegration in the radiation fields surrounding the neutron star: in the nebular region at the interface between the

---

<sup>2</sup> In the case when the conversion is not fully efficient, stochastic types of acceleration could take place at the shock to further push the maximum acceleration energy to the confinement limit  $\gamma_{\text{conf}} = ZeB_{\text{PWN}}R_{\text{PWN}}/(Am_p c^2)$  (where  $B_{\text{PWN}}$  and  $R_{\text{PWN}}$  represent respectively the pulsar wind nebula magnetic field and radius), which can reach values  $> 10^{11}$  over the spin-down timescale for neutron stars with parameters  $B \gtrsim 10^{12} \text{ G}$  and initial rotation period  $P_i \sim 1 \text{ ms}$  [36]. See however our discussion on acceleration limits due to synchrotron cooling a few paragraphs below.

pulsar wind and the supernova shell (a non-thermal component), and in the supernova ejecta, where most of the incident non-thermal radiation is thermalized over short timescales [41].

For neutrino production, the effects of this non-thermal radiation background in the nebula can be neglected as long as the confinement time of UHECRs in this region  $t_{\text{conf,neb}}$  is shorter than the photo-hadronic interaction timescale  $t_{A\gamma,\text{neb}}$ . The most important contribution to pion-production will come from photons produced by synchrotron emission. The synchrotron photon density for nebulae of fast-spinning neutron stars,  $n_\gamma$ , can be computed following Ref. [36], and the corresponding interaction timescale reads  $t_{A\gamma,\text{neb}} = (\sigma_{A\gamma} n_\gamma c)^{-1}$ , where  $\sigma_{A\gamma}$  is the photo-hadronic interaction cross-section. The magnetic confinement timescale in the nebula can be expressed  $t_{\text{conf,neb}} = R_{\text{neb}}^2 / (r_L c)$ , assuming a Bohm diffusion regime in the nebula magnetic field of strength  $B_{\text{neb}}$ .

These timescales depend on the size and on the average strength of the magnetic field in the expanding nebula region. These quantities can be calculated applying the estimates of Ref. [42] (see also [36, 41]). Figure 1 illustrates that the ratio  $t_{\text{conf,neb}}/t_{A\gamma,\text{neb}} \ll 1$  for fast-spinning pulsars and magnetars. This is in particular valid at times close to  $t_{\text{sd}}$  (vertical dotted lines) when most of the neutron star luminosity is provided. In the calculations, we have chosen  $\eta_B = 0.1$ , a parameter corresponding to the magnetic fraction of the energy injected into the nebula (and that is actually contained in  $\eta$  in Eq. 2.1). This value is rather conservative as  $\eta_B \ll 1$  from the observations of pulsar wind nebulae (e.g., [43–48]). These figures were computed for a particle Lorentz factor of  $10^9$ , but lower energies would lead to even milder effects of the radiation field.

As was pointed out in Ref. [41], it is thus possible that the UHECRs cross the nebula region without undergoing efficient photo-hadronic interactions. This remains valid except for strongly magnetized neutron stars. Note that protons would also cool via synchrotron in the strong magnetic field of the nebula, then particles would not reach very high energies for strongly magnetized magnetars [36]. However, UHECRs could interact with the radiation field of the supernova and produce ultrahigh energy neutrons that are not affected by synchrotron cooling. Besides, the conversion of the wind electromagnetic energy to kinetic energy is often assumed to be efficient because of the observation of the Crab Nebula [35], but this is not certain at the early stages and in the types of objects we are considering. This point is further supported by the fact that the MHD theory is unable to reproduce an efficient conversion (the so-called  $\sigma$ -problem) [35]. This would imply that the magnetic energy density of turbulent fields could be small enough, where synchrotron cooling can be avoided. Another possibility is that in a typical Type Ibc supernova, the ejecta mass could be as small as  $\sim 2M_\odot$  so that the ejecta velocity is larger, creating a larger nebula size with milder magnetic fields. Therefore cosmic ray particles may avoid significant synchrotron losses and reach the highest energies.

Particles then enter the supernova ejecta. At times shorter or of order the spin-down time  $t_{\text{sd}}$  that we consider here, the supernova ejecta is dense enough to provide a non-negligible interaction medium for the accelerated cosmic rays. In particular, the incident non-thermal radiation field from the nebula is nearly immediately thermalized and provide a thermal radiation background for photo-hadronic interactions.

The ejecta of a standard Type II core-collapse supernova can be modeled as a sphere ex-

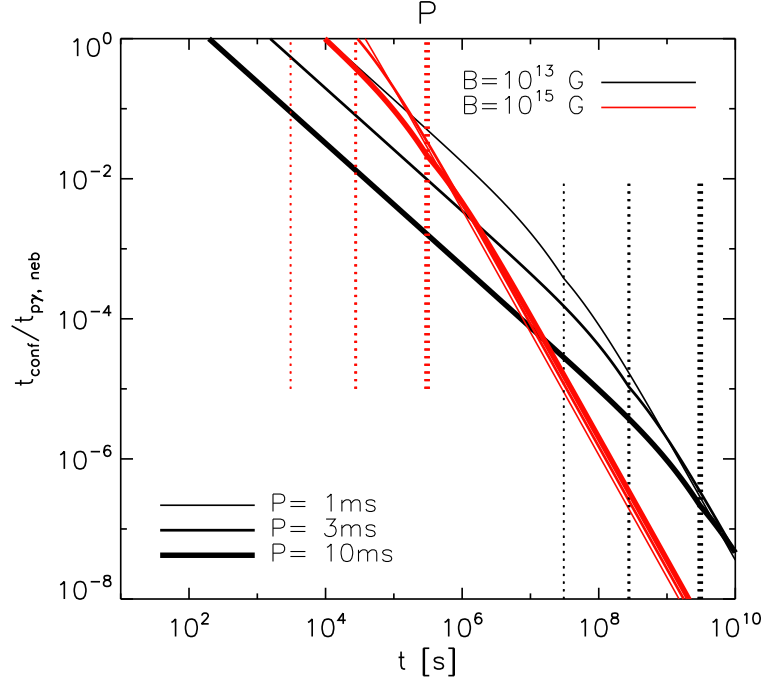


**Figure 1.** Time evolution of the ratio of the confinement timescale,  $t_{\text{conf}}$ , to the pion production timescale,  $t_{p\gamma}$ , in the non-thermal radiation field of the nebula region, for a proton at Lorentz factor  $10^9$ , for a neutron star with initial rotation period  $P_{-3} = 1, 3, 10$  (increasing thickness), dipole magnetic field  $B_{\star,13} = 1, 100$  (black and red), leptonic multiplicity  $\kappa_4 = 1$  and  $\eta_B = 0.1$ . The vertical dotted line indicates the spin-down timescale  $t_{\text{sd}}$  corresponding to each rotation period (increasing thickness).

panding with a velocity [41]

$$\beta_{\text{ej}} = \left( \frac{2E_{\text{SN}}}{M_{\text{ej}} c^2} \right)^{1/2} \left( 1 + \frac{E_{\text{rot}}}{E_{\text{SN}}} \right)^{1/2} \sim 4.8 \times 10^{-2} I_{45}^{1/2} P_{i,-3}^{-1} M_{\text{ej},1}^{-1/2}, \quad (2.8)$$

where the explosion energy of the supernova ejecta  $E_{\text{SN}} = 10^{51}$  erg and the pulsar wind energy  $E_{\text{rot}} = 2\pi^2 I / P_i^2$ . The size of the ejecta can be written as  $R_{\text{ej}}(t) = \beta_{\text{ej}} ct$ . Notice that for clarity, from here on we do not show the dependence of the numerical estimates on the inertia and the star radius (set to  $I_{45}$  and  $R_{\star,6}$  respectively), as these quantities are well-fixed by neutron star physics.

The thermal photon energy density in the supernova ejecta  $U_{\text{th}}$  reads

$$U_{\text{th}} = \frac{3 E_{\text{th}}}{4\pi R_{\text{ej}}^3} \quad (2.9)$$

where  $E_{\text{th}} = E_{\text{SN,th}} + \eta_{\text{th}} E_{\text{rot}}$ , with  $E_{\text{SN,th}} \sim 10^{49}$  erg being the thermal energy from the heating by supernova shocks and unstable isotopes such as  $^{56}\text{Ni}$ , and  $\eta_{\text{th}}$  is the fraction of the rotational energy converted into thermal photons [49]. The corresponding ejecta temperature can be expressed  $T = (U_{\text{th}}/a)^{1/4}$ , where  $a$  is the radiation constant. This thermal component peaks at energy  $\epsilon_{\gamma,\text{th}} = kT$ . The thermal radiation background leads to a cooling time by

photo-pion interaction for a proton

$$t_{p\gamma,\text{th}} = \left( c \xi_{p\gamma} \sigma_{p\gamma} \frac{U_{\text{th}}}{\epsilon_{\gamma,\text{th}}} \right)^{-1} \sim 2.5 \times 10^{-4} \text{ s } \eta_{\text{th},-2}^{-3/4} P_{\text{i},-3}^{-3/4} M_{\text{ej},1}^{-9/8} t_{3.5}^{9/4} \quad (2.10)$$

where  $\sigma_{p\gamma} \sim 5 \times 10^{-28} \text{ cm}^2$ , and the elasticity of the  $p\gamma$  interaction  $\xi_{p\gamma} = 0.2$  [14]. In this calculation, we have assumed that the particle energy lies always above photo-pion interaction threshold (and not in the resonance peak of the  $p\gamma$  interaction cross-section). For analytical estimations here and in the rest of this section, we have assumed parameters for which the pulsar rotational energy dominates the supernova intrinsic thermal energy.

The opacity then reads

$$\tau_{p\gamma,\text{th}} = \frac{R_{\text{ej}}}{ct_{p\gamma}} \sim 6.0 \times 10^5 \eta_{\text{th},-2}^{3/4} P_{\text{i},-3}^{-1/4} M_{\text{ej},1}^{5/8} t_{3.5}^{-5/4} , \quad (2.11)$$

and the time at which the medium becomes transparent to protons

$$t_{p\gamma,\text{th}}^* \equiv t(\tau_{p\gamma,\text{th}} = 1) \sim 1.3 \times 10^8 \text{ s } \eta_{\text{th},-2}^{3/5} P_{\text{i},-3}^{-1/5} M_{\text{ej},1}^{1/2} . \quad (2.12)$$

From these estimates, one can see that contrarily to the non-thermal radiation field in the nebula, the thermal radiative background in the supernova ejecta should have a strong effect on the accelerated particles at early times. Only a considerably small value of  $\eta_{\text{th}}$  would minimize its effect.

Cosmic ray energy at time  $t_{p\gamma,\text{th}}^*$  reads

$$E_{\text{CR}}(t = t_{p\gamma,\text{th}}^*) = 5.7 \times 10^{15} \text{ eV } A \eta \kappa_4 B_{15}^{-1} \eta_{\text{th},-2}^{-3/5} P_{\text{i},-3}^{1/5} M_{\text{ej},1}^{-1/2} . \quad (2.13)$$

We define

$$t_{p\gamma} \equiv \min(t_{p\gamma,\text{th}}, t_{p\gamma,\text{neb}}) , \quad (2.14)$$

its corresponding opacity  $\tau_{p\gamma}$ , and the time at which the medium becomes transparent for protons  $t_{p\gamma}^* \equiv t(\tau_{p\gamma} = 1)$ . From the above discussion,  $t_{p\gamma}^* \sim t_{p\gamma,\text{th}}^*$ .

### 2.3 Surrounding ejecta and escape (baryonic background)

At early times, the supernova ejecta presents also a dense baryonic background that can lead to efficient hadronic interactions for UHECRs. The mean density of the sphere over the size  $R_{\text{ej}}(t) = \beta_{\text{ej}} ct$  can be written [42]:

$$\rho_{\text{ej}}(t) = \frac{3 M_{\text{ej}}}{4\pi \beta_{\text{ej}}^3 c^3 t^3} \sim 5.1 \times 10^{-5} M_{\text{ej},1}^{5/2} P_{\text{i},-3}^3 t_{3.5}^{-3} \text{ g cm}^{-3} . \quad (2.15)$$

Here  $M_{\text{ej}} = 10 M_{\text{ej},1} M_{\odot}$  denotes the ejecta mass and  $E_{\text{ej}} = E_{\text{rot}} + E_{\text{exp}} \sim 2 \times 10^{52} \text{ erg } I_{45} P_{\text{i},-3}^{-2}$  the ejecta energy, expressed as the sum of the neutron star rotational energy and the supernova explosion energy ( $E_{\text{exp}} \sim 10^{51} \text{ erg}$ ) [50]. Equation (2.15) provides a reasonable estimate



of the evolution of the density of the ejecta surrounding the neutron star for various supernova scenarios, as is discussed in Ref. [16]. Note that results are only mildly sensitive to the ejecta mass within a range  $5 - 20 M_\odot$ .

As discussed in Ref. [16], the composition of the supernova ejecta depends upon the type, progenitor mass, and the final interior mass of the supernova, and rotation-powered pulsars and magnetars have been invoked as the remnant of a wide variety of supernova types, such as Ib, Ic, or II. The composition of all these objects is dominated by Hydrogen or light elements. For simplicity, we will consider in the following that the ejecta is composed of pure Hydrogen. We have demonstrated in Ref. [16] that different ejecta composition did not have a considerable impact as far as the production and escape of UHECRs was concerned.

The hadronic interaction timescale can be expressed as

$$t_{pp} = m_p (c \rho_{ej} \sigma_{pp} \xi_{pp})^{-1} \sim 1.7 \times 10^{-5} \text{ s } M_{ej,1}^{-5/2} P_{i,-3}^{-3} t_{3.5}^3, \quad (2.16)$$

and the background optical depth for protons

$$\tau_{pp} = \frac{R_{ej}}{c t_{pp}} \sim 8.9 \times 10^6 M_{ej,1}^2 P_{i,-3}^2 t_{3.5}^{-2}, \quad (2.17)$$

with the proton-proton interaction cross-section  $\sigma_{pp} \approx 1 \times 10^{-25} \text{ cm}^2$  at  $10^{18} \text{ eV}$  and  $\xi_{pp} \sim 0.5$ . Note that, at a given time, this quantity does not depend on the magnetic field of the neutron star. The dependence is actually implicitly considered, as we will evaluate the optical depth at time  $t_{sd}$ , which is shorter for faster spin-downs, i.e., for higher  $B$ . The corresponding time and energy at which cosmic rays can escape read

$$t_{pp}^* \equiv t(\tau_{pp} = 1) \sim 9.4 \times 10^6 \text{ s } M_{ej,1} P_{i,-3}. \quad (2.18)$$

$$E_{CR}(t = t_{pp}^*) \sim 6.0 \times 10^{16} \text{ eV } \eta \kappa P_{i,-3}^{-1} B_{15}^{-1} M_{ej,1}^{-1}. \quad (2.19)$$

This equation shows that, as was demonstrated and discussed in Refs. [12, 16], the ejecta is too dense to allow the escape of the highest energy protons through the supernova ejecta. For milder magnetic fields than for magnetars, the spin-down time is longer and the ejecta can become diluted enough to allow the escape of heavy nuclei at UHE. One might consider however that some mechanisms invoked in the next section and in Section 4 can carve a path for cosmic rays to escape safely, for magnetars in particular which are extreme objects.

## 2.4 Neutrino production and diffuse flux

The cosmic-ray interactions on the hadronic and radiative backgrounds described in the previous sections will inevitably lead to the production of charged pions, and thus of neutrinos. The meson production efficiency reads

$$f_{mes} = \min(\tau_{pp} + \tau_{p\gamma}, 1) \quad (2.20)$$

We will assume that for each interaction, charged pions undertake a fraction of the parent cosmic-ray energy  $f_\pi \equiv E_\pi/E_{CR} \sim 0.2$ , and each neutrino  $f_\nu \equiv E_\nu/E_\pi \sim 0.25$ .

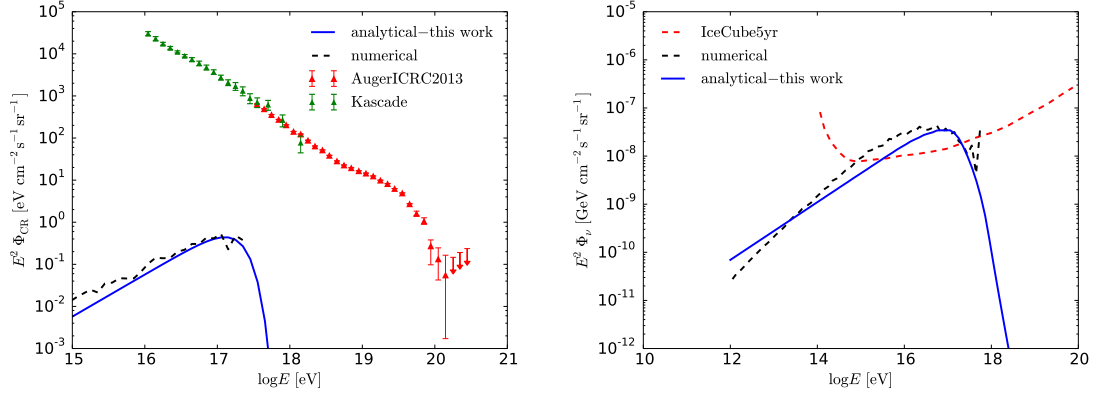


**Figure 2.** Spectra of cosmic rays (left) and neutrinos (right) from a magnetar with surface magnetic field  $B = 10^{15}$  G and initial spin period  $P_i = 1$  ms, comparing to measurements of the KASCADE [51, 52] and the Auger Observatory [53], as well as the IceCube 5-year sensitivity [54, 55]. Only hadronuclear interaction is taken into account, and the acceleration efficiency is set to be  $\eta = 1$ . In both plots, analytical results from this work (blue) are comparable to numerical results from [16, 56] (note that in the right panel, the black dashed line shows only neutrinos from primary cosmic rays).

At early times when the ejecta is very dense, the secondary nuclei and pions continue to interact with the radiation and hadron background and produce higher order nuclei, neutrinos and pions [14]. Charged pions have a lifetime of  $\tau_\pi = 2.6 \times 10^{-8}$  s in the lab frame. They interact with protons with cross section  $\sigma_{\pi p} \sim 5 \times 10^{-26}$  cm<sup>2</sup> and elasticity  $\xi_{\pi p} = 0.5$  [14], and with thermal photons with  $\sigma_{\pi\gamma} \sim 10^{-28}$  cm<sup>2</sup> and  $\xi_{\pi\gamma} \sim 0.5$ , producing additional neutrinos and pions that undergo further  $\pi p$  and  $\pi\gamma$  interaction. Notice that the  $\pi\gamma$  cross section was estimated by  $\sigma_{\pi\gamma} \sim \sigma_{p\gamma}(\sigma_{\pi p}/\sigma_{pp})$ . This cascade continues until  $\min(t_{\pi\gamma}, t_{\pi p}) = \gamma_\pi \tau_\pi$ . Charged pions then stop interacting and decay into neutrinos via  $\pi^\pm \rightarrow e^\pm + \nu_e(\bar{\nu}_e) + \bar{\nu}_\mu + \nu_\mu$ . One can then define a neutrino flux suppression factor as

$$f_{\text{sup}} = \min \left[ 1, \left( \left( \frac{t_{\pi p}}{\gamma_\pi \tau_\pi} \right)^{-1} + \left( \frac{t_{\pi\gamma}}{\gamma_\pi \tau_\pi} \right)^{-1} \right)^{-1} \right] \sim 6.5 \times 10^{-8} \eta^{-1} \kappa_4^{-1} P_{i,-3}^{-3} B_{15} M_{\text{ej},1}^{-5/2} t_{3.5}^4. \quad (2.21)$$

Assuming that cosmic rays follow  $dN_{\text{CR}}/dE_{\text{CR}} \propto E_{\text{CR}}^{-p}$ , then the spectrum of the neutrinos from the pion decay can be written as [14]:

$$E_\nu^2 \frac{dN_\nu}{dE_\nu} \propto \begin{cases} (E_\nu/E_\nu^{\text{had}})^{(2-p)} & \text{if } E_\nu < E_\nu^{\text{had}} \\ (E_\nu/E_\nu^{\text{had}})^{(1-p)} e^{-E_\nu/(f_\nu E_{\text{CR}})} & \text{if } E_\nu^{\text{had}} < E_\nu < E_{\text{CR}}/4 \end{cases} \quad (2.22)$$

where  $E_\nu^{\text{had}} \approx 0.25 (t_{\pi p}(E_{\text{CR}})/\tau_\pi) m_\pi c^2$  is the break energy for cosmic rays injected with energy  $E_{\text{CR}}$ . The neutrino flux is normalized by

$$\int E_\nu \frac{dN_\nu}{dE_\nu} dE_\nu = \int \frac{3}{8} E_{\text{CR}} \frac{dN_{\text{CR}}}{dE_{\text{CR}}} f_{\text{sup}} f_{\text{mes}} dE_{\text{CR}}. \quad (2.23)$$

The total neutrino spectrum thus breaks for  $f_{\text{sup}} = 1$  at time

$$t_{\nu,b} = 3.0 \times 10^5 \text{ s } \eta^{1/4} \kappa_4^{1/4} P_{i,-3}^{3/4} B_{15}^{-1/4} M_{\text{ej},1}^{5/8} \quad (2.24)$$

and at energy

$$E_{\nu,b} = 1.2 \times 10^{17} \text{ eV } A \kappa_4^{3/4} \eta^{3/4} P_{i,-3}^{-3/4} B_{15}^{-3/4} M_{\text{ej},1}^{-5/8} . \quad (2.25)$$

For the two estimates above, we have assume that  $\pi p$  interactions are dominant over  $\pi\gamma$ , as  $t_{\pi p} < t_{\pi\gamma}$  for our chosen parameters  $t_{3.5}$ ,  $B_{15}$  and  $P_{i,-3}$ . Note that most of the neutrinos are produced by cosmic rays of  $10^{18-19}$  eVs. The neutrino flux at the break energy from a population of UHECR sources with birth rate  $\mathfrak{R}(D)$  at a given distance  $D$ , can be estimated as

$$E_{\nu,b}^2 \Phi_{\nu,b} = \frac{1}{4\pi} \mathfrak{R}(0) f_z D_H \frac{3}{8} E_{\text{CR}}^2 \frac{dN_{\text{CR}}}{dE}(t_{\nu,b}) f_{\text{sup}} f_{\text{mes}} \quad (2.26)$$

where  $D_H$  is the Hubble distance corresponding to redshift  $z_H$ , and the factor

$$f_z \equiv \frac{1}{D_H} \int_0^{z_H} \frac{1}{1+z} \frac{dD}{dz} \frac{\mathfrak{R}(D)}{\mathfrak{R}(0)} dz . \quad (2.27)$$

For a uniform source birthrate  $\mathfrak{R}(D) = \mathfrak{R}(0)$ ,  $f_z \sim 0.55$ , and for a source emissivity following the star formation rate (SFR) as in Ref. [57],  $f_z \sim 2.5$ . For magnetars, for which hadronic interactions dominate, the diffuse neutrino flux can then be estimated as [14] (assuming  $t_{\text{sd}} \ll t_{\nu,b}$ )

$$\begin{aligned} E_{\nu,b}^2 \Phi_{\nu,b} &= 1.5 \times 10^{-8} \text{ GeV cm}^{-2} \text{ s}^{-1} \text{ sr}^{-1} \kappa_4^{3/4} P_{i,-3}^{-3/4} \eta^{3/4} B_{15}^{-7/4} Z^{-1} M_{\text{ej},1}^{-5/8} \\ &\times \frac{f_z}{2.25} \frac{\mathfrak{R}(0)}{1.2 \times 10^3 \text{ Gpc}^{-3} \text{ yr}^{-1}} . \end{aligned} \quad (2.28)$$

We normalize the flux of neutrinos by setting the associated cosmic-ray flux to the observed level. Assuming an energy loss length  $D_{\text{loss}}$  on the intergalactic backgrounds at a given energy, the cosmic-ray flux can be estimated roughly as

$$\Phi_{\text{CR}} \simeq \frac{1}{4\pi} E_{\text{CR}}^2 \frac{dN_{\text{CR}}}{dE_{\text{CR}}} \mathfrak{R}(0) D_{\text{loss}} . \quad (2.29)$$

At the cosmic-ray break energy, at time  $t_{\text{CR},b} = \max(t_{pp}^*, t_{p\gamma}^*) \sim t_{p\gamma}^*$ , the cosmic-ray flux thus reads

$$\begin{aligned} E_{\text{CR},b}^2 \Phi_{\text{CR}} &= 3.2 \times 10^{-11} \text{ GeV cm}^{-2} \text{ s}^{-1} \text{ sr}^{-1} A Z^{-1} \eta B_{15}^{-2} \kappa_4 \\ &\eta_{\text{th},-2}^{-3/5} P_{i,-3}^{1/5} M_{\text{ej},1}^{-1/2} \frac{\mathfrak{R}(0)}{1.2 \times 10^3 \text{ Gpc}^{-3} \text{ yr}^{-1}} \frac{D_{\text{loss}}}{4000 \text{ Mpc}} \end{aligned} \quad (2.30)$$

In the majority of the parameter-space considered,  $E_{\text{CR},pp} \lesssim 10^{17}$  eV and we fall in a regime where the energy-loss distance is close to the Hubble distance. Diffusion effects in the intergalactic magnetic fields would alter the distance  $D_{\text{loss}}$  (see, e.g., [58–60]) significantly for cosmic-ray energies  $\gtrsim 10^{17}$  eV, then we take the corresponding  $D_{\text{loss}}$  as calculated in [10].

In Figure 2 we show the cosmic ray and neutrino spectra from a magnetar with  $B = 10^{15}$  G and  $P_i = 1$  ms calculated using the above methods. As a consistency check, we also show the spectra calculated via numerical simulations [16, 56]. We find that the two approaches produce comparable results.

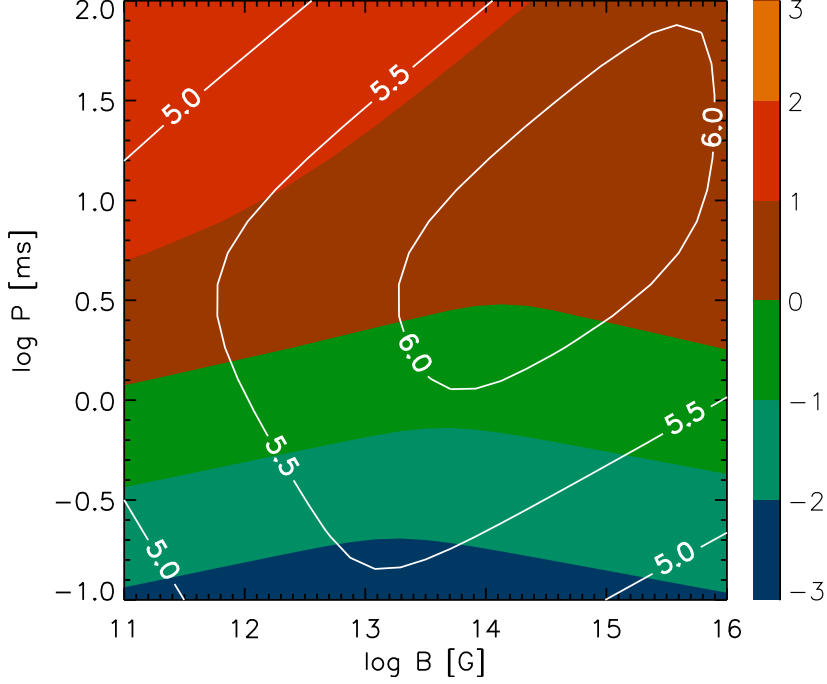


**Figure 3.** Interaction timescale ratios  $t_{p\gamma}/t_{pp}$  (colored contours) calculated at the break time  $t_{\nu,b}$  defined in Equation 2.24 (white contours showing  $\log t_{\nu,b}$ ), for the parameter space  $(B, P_i)$ , with  $\eta_{\text{th}} = 0.01$ . The radiation field is dominant over the hadronic backgrounds for the fastest-spinning neutron stars with sub-millisecond periods (green colors). For pulsars with periods more than  $\sim 1$  ms, hadronic interactions dominate at  $t_{\nu,b}$  (red colors).

The predicted flux is then compared with the observed cosmic ray flux  $\Phi_{\text{CR}}^{\text{ob}}$ . In our calculation we take the measurements by KASCADE [51, 52] and the Auger Observatory [53]. Notice that the energy losses by interactions on the cosmic radiation fields during the propagation from the source to the Earth further changes the spectrum. This change is not taken into account here, as the dominant process at these energies are adiabatic losses.

As the main contributors to cosmic rays below  $10^{17}$  eV are known to be most probably not extragalactic, we thus only consider sources that have the energetics to go above this energy, with  $E_0 = 10^{17}$  eV. This will be indicated as a green dashed line in the top left corner of our limiting contours in Sec. 3.

In addition, we limit the upper bound of the birth rate of the sources to be no more than 20% of supernova birth rate  $R_{\text{SN}} = 1.2 \times 10^5 \text{ Gpc}^{-3} \text{ yr}^{-1}$  [14, 61], which can be expressed

$$\mathfrak{R}(0) = \min \left( \frac{\Phi_{\text{CR}}^{\text{ob}}}{\Phi_{\text{CR}}} R_0, 20\% R_{\text{SN}} \right). \quad (2.31)$$

## 2.5 Comparison between radiative and hadronic background effects

As both radiative and hadronic backgrounds evolve with time, the dominant process in a pulsar also changes over time. The time  $t_{\nu,b}$  when neutrino spectrum breaks due to the ending of  $\pi p$  or  $\pi\gamma$  suppression (defined in Equation 2.24) serves as a good reference time for

the system. Figure 3 presents the ratios  $t_{pp}/t_{p\gamma}$  (colored contours) calculated at  $t_{\nu,b}$  (white contours showing  $\log t_{\nu,b}$ ), for the parameter space  $(B, P_i)$ , with  $\eta_{th} = 0.01$ . The radiation field is dominant over the hadronic backgrounds for the fastest-spinning neutron stars with spin period less than  $\sim 1$  ms. This is because the higher rotational speed the star has, the more energy can be converted to the thermal photons. To have hadronic interactions always dominate over photopion interactions over the entire  $(P, B)$  parameter-space studied here,  $\eta_{th}$  needs to be as low as  $\sim 10^{-6}$ . Our calculation here does consider super-luminous supernova. For super-luminous cases, the radiation energy can reach  $10^{51}$  erg, and the  $p\gamma$  process would be more important.

Note however that this calculation assumes that the radiation background in the supernova ejecta is isotropic. In the case of a jet-like structure, the radiation field would be beamed and the corresponding photon energy experienced by the proton would scale with  $1/\Gamma$ ,  $\Gamma$  being the Lorentz factor of the jet. For lower dissipation efficiency into radiation and beamed radiation, the contribution of the radiative background should be lower unless jet emission is intense. It is thus likely that the hadronic interactions are dominant over a large fraction of the parameter space that enables the acceleration of particles to UHE. This case is discussed in Section 4.

One caveat of this comparison assumes that accelerated cosmic rays undergo interactions with radiative and baryonic backgrounds at the same time. However in a realistic picture, cosmic rays would most probably interact with the thermal photons that fill the entire pulsar wind bubble first, and then with baryons when they manage to go through the bubble. In that case, the region filled with warm color in Fig. 3 should still be significantly impacted by the photopion process.

### 3 Parameter scan and the viable neutron stars

Figures 4 and 5 show the expected neutrino flux  $\log_{10}(E_{\nu,b}^2 \Phi_{\nu,b})$  emitted by populations of neutron stars over the parameter space of  $(B, P)$ , considering only hadronic interactions (Fig. 4) and both hadronic and photo-pion interactions (Fig. 5). In this parameter scan we assume that neutron stars have an acceleration efficiency  $\eta = 1$ , ejecta mass  $M_{ej} = 10 M_{\odot}$ , and a source emissivity following a uniform distribution. In these plots we have calibrated the source birthrate using cosmic ray observations. Specifically, for each point in the parameter space, the birth rate of the neutron star population with characteristics  $(P, B)$  is calculated so as to fit the measured cosmic ray flux at  $E_{CR,b}$ , following Eq. (2.31).

We first consider hadronic interactions in Fig. 4. The white contours present the neutrino break energy  $E_{\nu,b}$  where the neutrino spectrum peaks, and the green contours present the peak energies  $E_{CR,b}$  of high-energy cosmic rays from the neutron stars.  $E_{\nu,b}$  reaches  $10^{18}$  eV in the parameter region of  $10^{12} \text{ G} < B < 10^{15} \text{ G}$  and  $P_i < 0.6 \text{ ms}$ . For larger  $P$  and smaller  $B$ ,  $E_{\nu,b}$  decreases because the star is less energetic. On the other hand, when  $B > 10^{14} \text{ G}$ , magnetars have a fast spin-down time while the system remains too opaque for pions to decay, which results a cutoff on the neutrino peak energy. The dotted red line delimits the region where neutron stars would emit a diffusive neutrino background that exceeds the 5-year sensitivity of the IceCube Observatory.

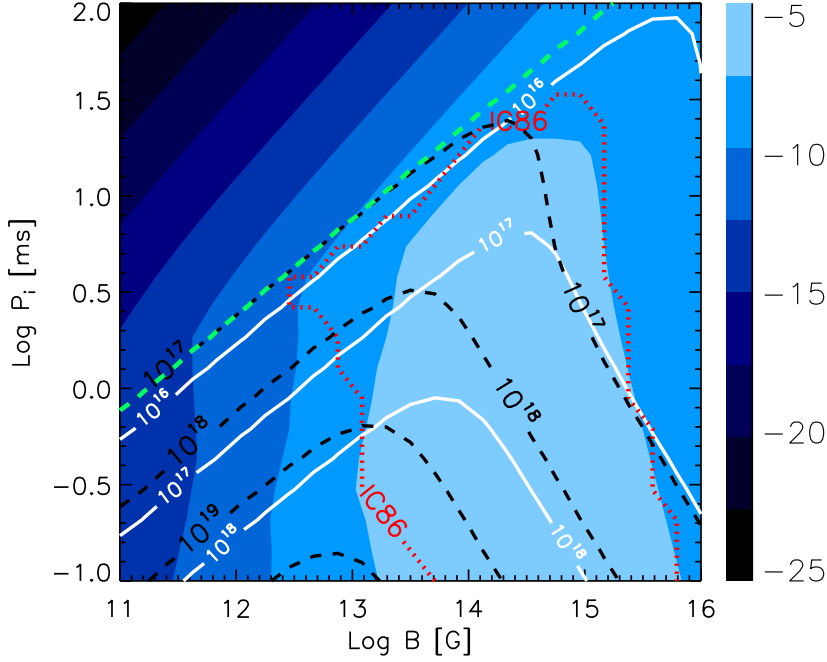


**Figure 4.** The neutrino flux  $\log_{10}(E_{\nu,b}^2 \Phi_{\nu,b})$  in  $\text{GeV cm}^{-2} \text{s}^{-1} \text{sr}^{-1}$  emitted by populations of neutron stars with the same characteristic  $(B, P)$ , assuming acceleration efficiency  $\eta = 1$ , ejecta mass  $M_{\text{ej}} = 10 M_{\odot}$ , jet fraction  $f_{\text{jet}} = 0$  and source emissivity following a SFR evolution. The sources birthrates are normalized via cosmic ray measurements. Only hadronic backgrounds is considered for the interactions. Overlaid are the IceCube 5-year sensitivity limit [54, 55] (red dotted), cosmic ray peak energies  $E_{\text{CR},b}$  (black dashed), and neutrino break energies  $E_{\nu,b}$  (white). We only consider parameter region below the green dashed line, which encloses sources that can produce cosmic rays above  $10^{17}$  eV. The parameter space below the red dotted line is excluded.

Figure 5 depicts the same parameter region, but additionally takes into account the radiation background in the pulsar winds. A thermalization factor of  $\eta_{\text{th}} = 0.01$  is assumed for this calculation. The radiation background does not change the neutrino break energy significantly. However, as the radiation field decreases much slower than the hadron background, it causes the cosmic ray spectrum to break much later in time compared to the hadronic case. As a result, the lower cosmic ray flux at  $E_{\text{CR},b}$  implies a higher normalization for the neutrino flux, and a larger parameter region is constrained by observations.

In Fig. 6 we present the limit contours for a range of acceleration efficiency with  $\eta = [0.01, 0.1, 0.5, 1]$ . For all four cases, we assume ejecta mass  $M_{\text{ej}} = 10 M_{\odot}$ , no jet configuration, and source emissivity following SFR. Both hadronic and radiation backgrounds with  $\eta_{\text{th}} = 0.01$  are considered. We find no strong variation in cases with  $\eta \geq 0.5$ . For  $\eta < 0.5$ , the confinement area decreases for smaller  $\eta$ . Note that in the case  $\eta = 0.01$ , the maximum cosmic ray energy accelerated by the pulsar wind can only reach  $10^{18}$  eV.

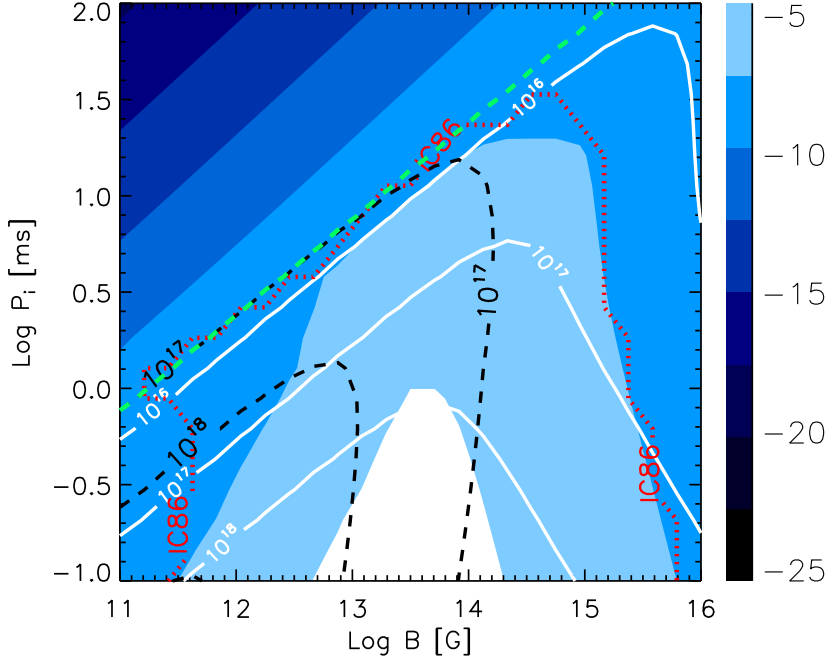


**Figure 5.** Same as Fig. 4, but considering both hadronic and radiative backgrounds. For the radiative background, we assume  $\eta_{\text{th}} = 0.01$ , and the thermal component dominants over the non-thermal component (see Sec. 2.2 for details).

#### 4 In presence of jet-like structures

The confining pressure of the toroidal magnetic field could collimate the proto-magnetar wind along its polar axis, and drive a jet that has the properties of long gamma-ray bursts jets [38, 62–66]. Cosmic rays accelerated inside the proto-magnetar jet could then escape through the pierced supernova envelope. The escape of nuclei through jets, taking into account the radiative and baryonic background fields, has been discussed semi-analytically in the context of GRBs by Ref. [67] and for proto-magnetar jets by Ref. [68].

The collimation power becomes significant for values of the ratio of the Poynting flux to the total energy at the termination shock of the wind,  $\dot{E}_{\text{mag}}/\dot{E}_{\text{tot}} \gtrsim 0.2$ , at times  $t \sim 10 - 100$  s [64]. The conversion of magnetic energy into kinetic energy in relativistic outflows at large radii are uncertain and might not allow the formation of a jet. Studies of the Crab Pulsar wind nebula show indeed that  $\dot{E}_{\text{mag}}/\dot{E}_{\text{tot}} \sim 10^{-2}$  at large radii [44, 69], but magnetars could have different fates.

Reference [13] also proposed that the supernova ejecta could be disrupted by the magnetar wind. Such phenomena have never been observed, neither in magnetar envelopes, nor in rotation-powered pulsar envelopes.

We parametrize the uncertainties of these escape scenarios by introducing the quantity  $f_{\text{jet}}$ , that gives the fraction of accelerated particles that can escape without crossing a dense environment. Note that even in the presence of a jet, particles injected off the jet-axis will still undergo interactions with the rest of the ejecta that has not been pierced.

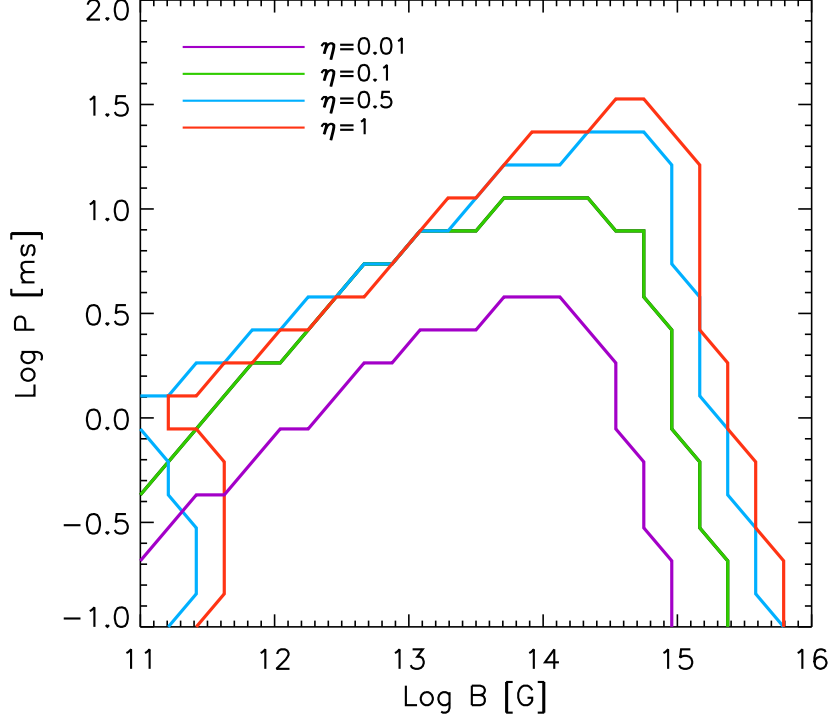


**Figure 6.** Limiting contours for different acceleration efficiency  $\eta = 0.01, 0.1, 0.5, 1$ . As in the previous plots, the parameter space below the contours is excluded by IceCube. All cases assume ejecta mass  $M_{\text{ej}} = 10 M_{\odot}$ , no jet and source emissivity following SFR evolution. The sources birthrates are normalized via cosmic ray measurements. Both hadronic backgrounds and radiative backgrounds assuming  $\eta_{\text{th}} = 0.01$  are considered for the interactions.

The flux of cosmic rays escaped from jets is compared to the observed cosmic ray flux, putting an extra constraint on the magnetar birth rate, in addition to that from the cosmic rays leave from the non-jet region after interactions:

$$\mathfrak{R}(0) = \min \left( \frac{\Phi_{\text{CR}}^{\text{ob}}}{\Phi_{\text{CR,sp}}} R_0, \frac{\Phi_{\text{CR}}^{\text{ob}}}{\Phi_{\text{CR,jet}}} R_0, 20\% R_{\text{SN}} \right) \quad (4.1)$$

where  $\Phi_{\text{CR,jet}} = f_{\text{jet}} E_0^2 dN/dE \mathfrak{R}(0) D_{\text{loss}}/4\pi$  is the cosmic ray flux from the jet region peaking at  $E_0$ , while  $\Phi_{\text{CR,sp}} = (1 - f_{\text{jet}}) \Phi_{\text{CR}}$  is the flux from the non-jet region peaking at  $E_{\text{CR,b}}$ .

Figure 7 presents the neutrino flux over the parameter space assuming a jet fraction  $f_{\text{jet}} = 0.1$ . The parameter region with  $B > 10^{14}$  G and  $P < 10$  ms is significantly impacted. The reason is that the jet allows the escape of UHECRs accelerated by the fast-spinning magnetars in this region, which poses a strong limit on the star burst rate due to their low flux. The constraints on magnetars with larger spin periods still hold.

Figure 8 shows the limiting contours for different jet fractions with  $f_{\text{jet}} = [0.001, 0.01, 0.1, 0.5]$ .  $\eta = 1$  and source emissivity following SFR have been assumed for all cases. As expected, when  $f_{\text{jet}} \ll 1$ , the results get back to cases without any jet configuration. The parameter space is less confined with a large  $f_{\text{jet}}$ , as most cosmic rays escape without producing neutrinos. Interestingly, the most standard magnetars remain excluded even with a large jet fraction.



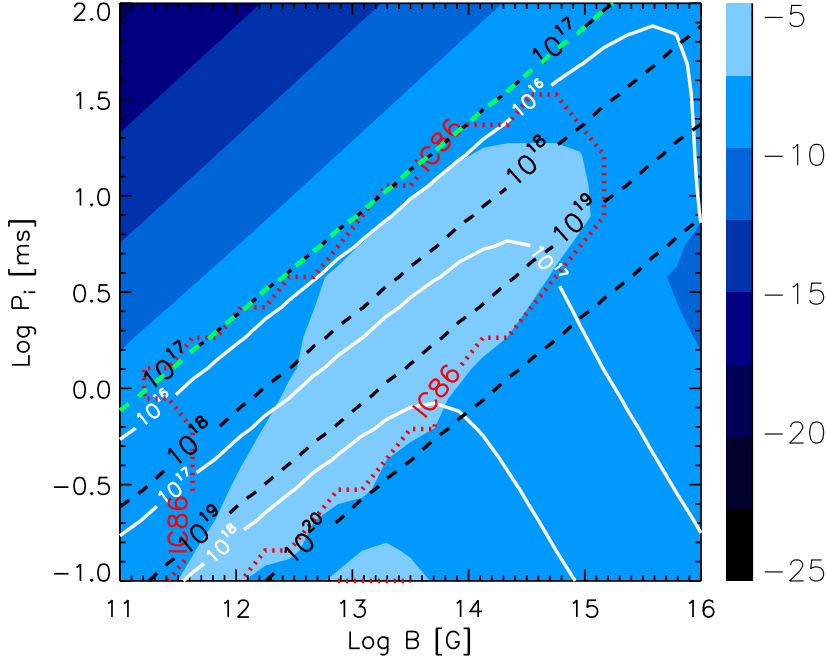


**Figure 7.** The neutrino flux  $\log_{10}(E_{\nu,b}^2 \Phi_{\nu,b})$  in  $\text{GeV cm}^{-2} \text{s}^{-1} \text{sr}^{-1}$  emitted by populations of neutron stars with the same characteristic  $(B, P)$ , assuming acceleration efficiency  $\eta = 1$ , ejecta mass  $M_{\text{ej}} = 10 M_{\odot}$ , jet fraction  $f_{\text{jet}} = 0.1$  and source emissivity following SFR. The sources birthrates are normalized via cosmic ray measurements. Both hadronic backgrounds and radiative backgrounds assuming  $\eta_{\text{th}} = 0.01$  are considered for the interactions. Overplotted are the IceCube sensitivity limit (red dotted), cosmic ray peak energy  $E_{\text{cr,peak}}$  (black dashed), and neutrino break energies  $E_{\nu,b}$  (white). The parameter space within the red dotted line is excluded.

## 5 Discussion, conclusions

In this work we have constrained magnetars as sources of cosmic rays above  $10^{17} \text{eV}$ , by comparing their expected neutrino production to the observational limits measured by the IceCube Observatory. We have considered particle interactions with both radiative field in the pulsar wind nebula and the hadronic backgrounds of the supernova ejecta. High-energy neutrinos provide a powerful tool to probe very high-energy cosmic-ray acceleration hidden in supernova ejecta [14]. Assuming a proton cosmic ray composition, we find that the assumption of magnetars being the dominant high-energy cosmic ray sources is mostly ruled out by the IceCube upper limits on the diffusive neutrino background, unless the ejecta mass is much smaller than in a typical core-collapse supernova, or a large fraction of cosmic rays can escape without significant interactions from the jet-like structures piercing the ejecta.

Throughout the work we have assumed that cosmic rays are mostly composed of protons. If cosmic rays are instead nuclei with mass number  $A$ , their meson production efficiency from interactions with hadronic backgrounds would decrease by  $f_{\text{mes},Np} \propto A^{-1/3}$  [31], while that from the photodisintegration drops to  $f_{\text{mes},p\gamma} \propto A^{-1.21}$  [70]. On the other hand, as Eq. (2.5) shows, nuclei would be accelerated at much later time than protons at the same energy. As a result, the environment would be less dense and particles could escape with higher energies compared to the proton scenario. In the end we would expect less neutrino production and a

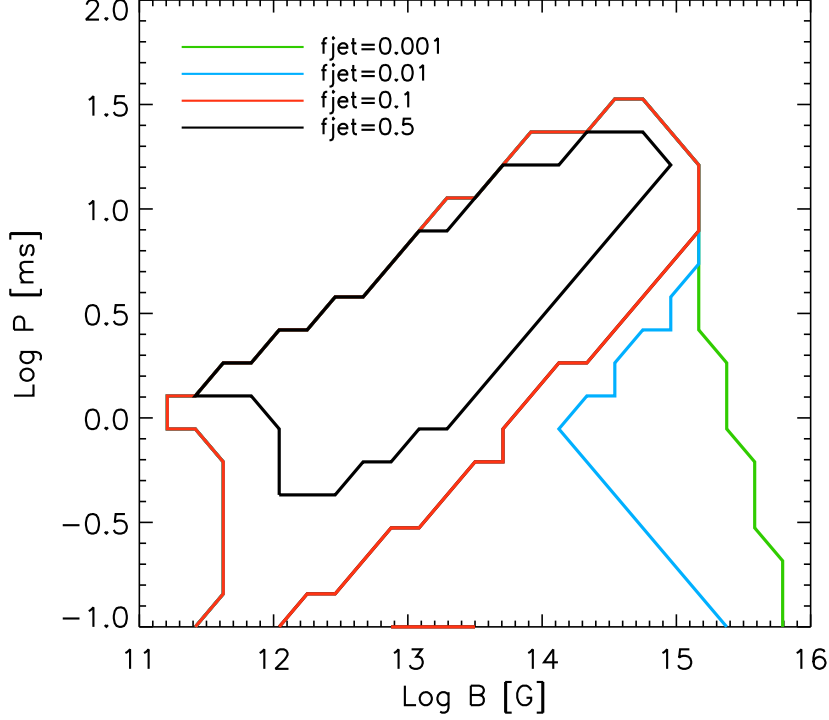


**Figure 8.** Limiting contours for different jet fraction  $f_{\text{jet}} = 0.001, 0.01, 0.1, 0.5$ . Like previous plots, the parameter space within the contours is excluded by IceCube. All cases assume ejecta mass  $M_{\text{ej}} = 10 M_{\odot}$ ,  $\eta = 1$  and source emissivity following SFR. The sources birthrates are normalized via cosmic ray measurements. Both hadronic backgrounds and radiative backgrounds assuming  $\eta_{\text{th}} = 0.01$  are considered for the interactions.

less constrained parameter space if cosmic rays have a heavy composition. However, we note that a large number of higher-order products, including secondary mesons and neutrinos, would also result from the  $Np$  and  $N\gamma$  interactions and thus help to constrain the parameter space. Indeed, as Ref. [31] shows, there is no significant difference between the neutrino flux produced by protons and iron nuclei primaries, if considering only hadronic interactions.

In Section 4, we showed that the presence of jets in magnetars enabling the escape of UHECRs can help remove the tension between their EeV neutrino productions and the observation. In particular, we demonstrate that if 10% cosmic rays can leak from the jet structure, fast-spinning magnetars shift outside of the exclusion region due to the IceCube limits, as the low UHECR flux ensures a rare magnetar birth rate.

Reference [71] suggested that neutron stars at birth have spin periods that follow a normal distribution with mean 300 ms and standard derivation 150 ms, and the log of their dipole magnetic fields that follow a normal distribution with mean 12.65 and standard derivation 0.55. Here we have ignored the effect of such a distribution as we aim to separate the contribution from different parts of the parameter space. In particular, we focus on magnetars in this work, and it is not obvious that these objects present such a distribution. Cosmic ray and neutrino productions from a cumulation of neutron star population following a  $(P, B)$  distribution can be found in [17, 31]. We stress that the conclusions of these works (that focus on mildly magnetized pulsars) are not in contradiction with the present paper, because

of the population distribution and the injection of a non-proton composition.

## References

- [1] C. J. Cesarsky, *Cosmic-ray confinement in the galaxy*, *Ann. Rev. Astron. Astrophys.* **18** (1980), no. 1 289–319, [<http://www.annualreviews.org/doi/pdf/10.1146/annurev.aa.18.090180.001445>].
- [2] A. M. Hillas, *The Origin of Ultra-High-Energy Cosmic Rays*, *ARAA* **22** (1984) 425–444.
- [3] A. W. Strong, I. V. Moskalenko, and V. S. Ptuskin, *Cosmic-ray propagation and interactions in the Galaxy*, *Ann. Rev. Nucl. Part. Sci.* **57** (2007) 285–327, [[astro-ph/0701517](#)].
- [4] M. Tavani, A. Giuliani, A. W. Chen, et al., *Direct Evidence for Hadronic Cosmic-Ray Acceleration in the Supernova Remnant IC 443*, *ApJ Lett.* **710** (Feb., 2010) L151–L155, [[arXiv:1001.5150](#)].
- [5] A. Giuliani, M. Cardillo, M. Tavani, Y. Fukui, et al., *Neutral Pion Emission from Accelerated Protons in the Supernova Remnant W44*, *ApJ Lett.* **742** (Dec., 2011) L30–L35, [[arXiv:1111.4868](#)].
- [6] M. Ackermann, M. Ajello, A. Allafort, et al., *Detection of the Characteristic Pion-Decay Signature in Supernova Remnants*, *Science* **339** (Feb., 2013) 807–811, [[arXiv:1302.3307](#)].
- [7] G. Giacinti, M. Kachelriess, D. Semikoz, and G. Sigl, *Ultrahigh Energy Nuclei in the Turbulent Galactic Magnetic Field*, *Astropart.Phys.* **35** (2011) 192–200, [[arXiv:1104.1141](#)].
- [8] Pierre Auger Collaboration, P. Abreu, M. Aglietta, M. Ahlers, E. J. Ahn, I. F. M. Albuquerque, D. Allard, I. Allekotte, J. Allen, P. Allison, and et al., *Search for Point-like Sources of Ultra-high Energy Neutrinos at the Pierre Auger Observatory and Improved Limit on the Diffuse Flux of Tau Neutrinos*, *ApJ Lett.* **755** (Aug., 2012) L4, [[arXiv:1210.3143](#)].
- [9] T. Telescope Array, Pierre Auger Collaborations, :, T. Abu-Zayyad, M. Allen, R. Anderson, R. Azuma, E. Barcikowski, J. W. Belz, D. R. Bergman, and et al., *Pierre Auger Observatory and Telescope Array: Joint Contributions to the 33rd International Cosmic Ray Conference (ICRC 2013)*, *ArXiv e-prints* (Oct., 2013) [[arXiv:1310.0647](#)].
- [10] K. Kotera and A. V. Olinto, *The Astrophysics of Ultrahigh Energy Cosmic Rays*, *Ann.Rev.Astron.Astrophys.* **49** (2011) 119–153, [[arXiv:1101.4256](#)].
- [11] A. Venkatesan, M. C. Miller, and A. V. Olinto, *Constraints on the Production of Ultra-High-Energy Cosmic Rays by Isolated Neutron Stars*, *ApJ* **484** (July, 1997) 323–+, [[astro-ph/](#)].
- [12] P. Blasi, R. I. Epstein, and A. V. Olinto, *Ultra-High-Energy Cosmic Rays from Young Neutron Star Winds*, *ApJ Letters* **533** (Apr., 2000) L123–L126.
- [13] J. Arons, *Magnetars in the Metagalaxy: An Origin for Ultra-High-Energy Cosmic Rays in the Nearby Universe*, *ApJ* **589** (June, 2003) 871–892.
- [14] K. Murase, P. Mészáros, and B. Zhang, *Probing the birth of fast rotating magnetars through high-energy neutrinos*, *Phys. Rev. D* **79** (May, 2009) 103001–+, [[arXiv:0904.2509](#)].
- [15] K. Kotera, *Ultrahigh energy cosmic ray acceleration in newly born magnetars and their associated gravitational wave signatures*, *Phys. Rev. D* **84** (July, 2011) 023002, [[arXiv:1106.3060](#)].
- [16] K. Fang, K. Kotera, and A. V. Olinto, *Newly Born Pulsars as Sources of Ultrahigh Energy Cosmic Rays*, *The Astrophysical Journal* **750** (May, 2012) 118, [[arXiv:1201.5197](#)].

- [17] K. Fang, K. Kotera, and A. V. Olinto, *Ultrahigh energy cosmic ray nuclei from extragalactic pulsars and the effect of their Galactic counterparts*, *JCAP* **3** (Mar., 2013) 10, [[arXiv:1302.4482](#)].
- [18] D. R. Lorimer, *Binary and millisecond pulsars*, *Living Reviews in Relativity* **11** (2008), no. 8.
- [19] K. Murase and H. Takami, *Implications of Ultra-High-Energy Cosmic Rays for Transient Sources in the Auger Era*, *Astrophys. J.* **690** (2009) L14–L17, [[arXiv:0810.1813](#)].
- [20] B. Katz, R. Budnik, and E. Waxman, *The energy production rate and the generation spectrum of UHECRs*, *Journal of Cosmology and Astro-Particle Physics* **3** (Mar., 2009) 20–+, [[arXiv:0811.3759](#)].
- [21] P. M. Woods and C. Thompson, *Soft gamma repeaters and anomalous X-ray pulsars: magnetar candidates*, pp. 547–586. In: *Compact stellar X-ray sources*. Edited by Walter Lewin & Michiel van der Klis. Cambridge Astrophysics Series, No. 39. Cambridge, UK: Cambridge University Press, ISBN 978-0-521-82659-4, Apr., 2006.
- [22] A. K. Harding and D. Lai, *Physics of strongly magnetized neutron stars*, *Reports on Progress in Physics* **69** (Sept., 2006) 2631–2708, [[astro-ph/](#)].
- [23] S. Mereghetti, *The strongest cosmic magnets: soft gamma-ray repeaters and anomalous X-ray pulsars*, *The Astronomy and Astrophysics Review* **15** (July, 2008) 225–287, [[arXiv:0804.0250](#)].
- [24] B. D. Metzger, D. Giannios, T. A. Thompson, N. Bucciantini, and E. Quataert, *The protomagnetar model for gamma-ray bursts*, *MNRAS* (Mar., 2011) 445–+.
- [25] R. C. Duncan and C. Thompson, *Formation of very strongly magnetized neutron stars - Implications for gamma-ray bursts*, *ApJ Letters* **392** (June, 1992) L9–L13.
- [26] C. Kouveliotou, S. Dieters, T. Strohmayer, J. van Paradijs, G. J. Fishman, C. A. Meegan, K. Hurley, J. Kommers, I. Smith, D. Frail, and T. Murakami, *An X-ray pulsar with a superstrong magnetic field in the soft  $\gamma$ -ray repeater SGR1806 - 20*, *Nature* **393** (May, 1998) 235–237.
- [27] C. Kouveliotou, T. Strohmayer, K. Hurley, J. van Paradijs, M. H. Finger, S. Dieters, P. Woods, C. Thompson, and R. C. Duncan, *Discovery of a Magnetar Associated with the Soft Gamma Repeater SGR 1900+14*, *ApJ Letters* **510** (Jan., 1999) L115–L118, [[astro-ph/](#)].
- [28] M. G. Baring and A. K. Harding, *Photon Splitting and Pair Creation in Highly Magnetized Pulsars*, *ApJ* **547** (Feb., 2001) 929–948, [[astro-ph/](#)].
- [29] P. Abreu et al., *The pierre auger observatory ii: Studies of cosmic ray composition and hadronic interaction models*, *32nd International Cosmic Ray Conference, Beijing, China* (2011) arXiv:1107.4804.
- [30] Y. Tameda et al. *32nd International Cosmic Ray Conference, Beijing, China* **2** (2011), no. 246.
- [31] K. Fang, K. Kotera, K. Murase, and A. V. Olinto, *A decisive test for the young pulsar origin of ultrahigh energy cosmic rays with IceCube*, *ArXiv e-prints* (Nov., 2013) [[arXiv:1311.2044](#)].
- [32] M. A. Ruderman and P. G. Sutherland, *Theory of pulsars - Polar caps, sparks, and coherent microwave radiation*, *ApJ* **196** (Feb., 1975) 51–72.
- [33] J. Arons and E. T. Scharlemann, *Pair formation above pulsar polar caps - Structure of the low altitude acceleration zone*, *ApJ* **231** (Aug., 1979) 854–879.
- [34] J. Arons, *Theory of Pulsar Winds*, in *Neutron Stars in Supernova Remnants* (P. O. Slane and B. M. Gaensler, eds.), vol. 271 of *Astronomical Society of the Pacific Conference Series*, p. 71, 2002.
- [35] J. G. Kirk, Y. Lyubarsky, and J. Petri, *The Theory of Pulsar Winds and Nebulae*, in *Astrophysics and Space Science Library* (W. Becker, ed.), vol. 357 of *Astrophysics and Space Science Library*, p. 421, 2009. [astro-ph/](#).

- [36] M. Lemoine, K. Kotera, and J. Pétri, *On ultra-high energy cosmic ray acceleration at the termination shock of young pulsar winds*, *ArXiv e-prints: 1409.0159* (Aug., 2014) [[arXiv:1409.0159](#)].
- [37] P. Goldreich and W. H. Julian, *Pulsar Electrodynamics*, *ApJ* **157** (Aug., 1969) 869.
- [38] V. V. Usov, *Millisecond pulsars with extremely strong magnetic fields as a cosmological source of gamma-ray bursts*, *Nature* **357** (June, 1992) 472–474.
- [39] S. Bonazzola and E. Gourgoulhon, *Gravitational waves from pulsars: emission by the magnetic-field-induced distortion.*, *A&A* **312** (Aug., 1996) 675–690, [[astro-ph/](#)].
- [40] J. P. Ostriker and J. E. Gunn, *On the Nature of Pulsars. I. Theory*, *ApJ* **157** (Sept., 1969) 1395–+.
- [41] K. Kotera, E. S. Phinney, and A. V. Olinto, *Signatures of pulsars in the light curves of newly formed supernova remnants*, *MNRAS* **432** (July, 2013) 3228–3236, [[arXiv:1304.5326](#)].
- [42] R. A. Chevalier, *Young Core-Collapse Supernova Remnants and Their Supernovae*, *ApJ* **619** (Feb., 2005) 839–855, [[astro-ph/](#)].
- [43] M. J. Rees and J. E. Gunn, *The origin of the magnetic field and relativistic particles in the Crab Nebula*, *MNRAS* **167** (Apr., 1974) 1–12.
- [44] C. F. Kennel and F. V. Coroniti, *Confinement of the Crab pulsar’s wind by its supernova remnant*, *ApJ* **283** (Aug., 1984) 694–709.
- [45] C. F. Kennel and F. V. Coroniti, *Magnetohydrodynamic model of Crab nebula radiation*, *ApJ* **283** (Aug., 1984) 710–730.
- [46] A. M. Atoyan and F. A. Aharonian, *On the mechanisms of gamma radiation in the Crab Nebula*, *MNRAS* **278** (Jan., 1996) 525–541.
- [47] L. Del Zanna, E. Amato, and N. Bucciantini, *Axially symmetric relativistic MHD simulations of Pulsar Wind Nebulae in Supernova Remnants. On the origin of torus and jet-like features*, *A&A* **421** (July, 2004) 1063–1073, [[astro-ph/](#)].
- [48] S. Komissarov and Y. Lyubarsky, *MHD Simulations of Crab’s Jet and Torus*, *Ap & SS* **293** (Sept., 2004) 107–113.
- [49] K. Murase, *High energy neutrino early afterglows gamma-ray bursts revisited*, *Phys.Rev.* **D76** (2007) 123001, [[arXiv:0707.1140](#)].
- [50] C. D. Matzner and C. F. McKee, *The Expulsion of Stellar Envelopes in Core-Collapse Supernovae*, *ApJ* **510** (Jan., 1999) 379–403, [[astro-ph/](#)].
- [51] W. Apel et al., *Kneelike structure in the spectrum of the heavy component of cosmic rays observed with KASCADE-Grande*, *Phys.Rev.Lett.* **107** (2011) 171104, [[arXiv:1107.5885](#)].
- [52] W. Apel, J. Arteaga-Velázquez, K. Bekk, M. Bertaina, J. Blümer, et al., *Ankle-like Feature in the Energy Spectrum of Light Elements of Cosmic Rays Observed with KASCADE-Grande*, *Phys.Rev.* **D87** (2013) 081101, [[arXiv:1304.7114](#)].
- [53] **Pierre Auger Collaboration** Collaboration, A. Aab et al., *The Pierre Auger Observatory: Contributions to the 33rd International Cosmic Ray Conference (ICRC 2013)*, [[arXiv:1307.5059](#)].
- [54] R. Abbasi et al., *The IceCube Neutrino Observatory II: All Sky Searches: Atmospheric, Diffuse and EHE*, [[arXiv:1111.2736](#)].
- [55] M. G. Aartsen, R. Abbasi, Y. Abdou, M. Ackermann, J. Adams, J. A. Aguilar, M. Ahlers, D. Altmann, J. Auffenberg, X. Bai, and et al., *Search for Time-independent Neutrino Emission from Astrophysical Sources with 3 yr of IceCube Data*, *ApJ* **779** (Dec., 2013) 132.

- [56] K. Fang, *High-energy neutrino signatures of newborn pulsars in the local universe*, *JCAP* **6** (June, 2015) 4, [[arXiv:1411.2174](#)].
- [57] A. M. Hopkins and J. F. Beacom, *On the Normalization of the Cosmic Star Formation History*, *ApJ* **651** (Nov., 2006) 142–154, [[astro-ph/0601463](#)].
- [58] M. Lemoine, *Extragalactic magnetic fields and the second knee in the cosmic-ray spectrum*, *Phys. Rev. D* **71** (Apr., 2005) 083007, [[0411173](#)].
- [59] K. Kotera and M. Lemoine, *Inhomogeneous extragalactic magnetic fields and the second knee in the cosmic ray spectrum*, *Phys. Rev. D* **77** (Jan., 2008) 023005, [[arXiv:0706.1891](#)].
- [60] K. Kotera and M. Lemoine, *Optical depth of the Universe to ultrahigh energy cosmic ray scattering in the magnetized large scale structure*, *Phys. Rev. D* **77** (June, 2008) 123003, [[arXiv:0801.1450](#)].
- [61] B. Zhang, Z. G. Dai, P. Mészáros, E. Waxman, and A. K. Harding, *High-Energy Neutrinos from Magnetars*, *ApJ* **595** (Sept., 2003) 346–351, [[astro-ph/0210382](#)].
- [62] T. A. Thompson, P. Chang, and E. Quataert, *Magnetar Spin-Down, Hyperenergetic Supernovae, and Gamma-Ray Bursts*, *ApJ* **611** (Aug., 2004) 380–393, [[astro-ph/0401555](#)].
- [63] S. S. Komissarov and M. V. Barkov, *Magnetar-energized supernova explosions and gamma-ray burst jets*, *MNRAS* **382** (Dec., 2007) 1029–1040, [[arXiv:0707.0264](#)].
- [64] N. Bucciantini, E. Quataert, J. Arons, B. D. Metzger, and T. A. Thompson, *Magnetar-driven bubbles and the origin of collimated outflows in gamma-ray bursts*, *MNRAS* **380** (Oct., 2007) 1541–1553, [[arXiv:0705.1742](#)].
- [65] N. Bucciantini, E. Quataert, J. Arons, B. D. Metzger, and T. A. Thompson, *Relativistic jets and long-duration gamma-ray bursts from the birth of magnetars*, *MNRAS* **383** (Jan., 2008) L25–L29, [[arXiv:0707.2100](#)].
- [66] N. Bucciantini, E. Quataert, B. D. Metzger, T. A. Thompson, J. Arons, and L. Del Zanna, *Magnetized relativistic jets and long-duration GRBs from magnetar spin-down during core-collapse supernovae*, *MNRAS* **396** (July, 2009) 2038–2050, [[arXiv:0901.3801](#)].
- [67] K. Murase, K. Ioka, S. Nagataki, and T. Nakamura, *High-energy cosmic-ray nuclei from high- and low-luminosity gamma-ray bursts and implications for multimessenger astronomy*, *Phys. Rev. D* **78** (July, 2008) 023005–+, [[arXiv:0801.2861](#)].
- [68] B. D. Metzger, D. Giannios, and S. Horiuchi, *Heavy nuclei synthesized in gamma-ray burst outflows as the source of ultrahigh energy cosmic rays*, *MNRAS* **415** (Aug., 2011) 2495–2504, [[arXiv:1101.4019](#)].
- [69] M. C. Begelman and Z.-Y. Li, *An axisymmetric magnetohydrodynamic model for the Crab pulsar wind bubble*, *ApJ* **397** (Sept., 1992) 187–195.
- [70] K. Murase and J. F. Beacom, *Neutrino Background Flux from Sources of Ultrahigh-Energy Cosmic-Ray Nuclei*, *Phys.Rev.* **D81** (2010) 123001, [[arXiv:1003.4959](#)].
- [71] C.-A. Faucher-Giguère and V. M. Kaspi, *Birth and Evolution of Isolated Radio Pulsars*, *ApJ* **643** (May, 2006) 332–355.